Beam Dynamics Corrections to Measurements of the Muon Anomalous Magnetic Moment

On Kim[a,1,*] **for the Muon** $g-2$ **Collaboration**

[a]*University of Mississippi,
University, MS 38677, USA*

E-mail: okim@olemiss.edu

The Muon $g-2$ experiment at Fermilab is making progress towards its physics goal of measuring the muon anomalous magnetic moment with the unprecedented precision of 140 parts per billion. In April 2021, the collaboration published the first measurement based on the first year of data taking. The second result is based on the second and third years of data taking combined. We discuss the corrections to the anomalous spin precession signal due to beam dynamics effects being used to determine the anomalous spin precession frequency for the second result.

---

[*]Speaker

---

1. Introduction

The Muon $g - 2$ experiment at Fermilab measures the magnetic anomaly of the muon (a_μ) to unprecedented precision, 140 parts per billion (ppb). Its first result, which was based on the data taken in 2018, was consistent with the predecessor experiment at Brookhaven National Laboratory, and the tension between the experimental average of a_μ and the Standard Model prediction reached 4.2 standard deviations [1]. The new results based on 2019 and 2020 data that came out this August agreed again well with the previous measurements with the improved uncertainty by a factor of two [2], as shown in Fig. 1.
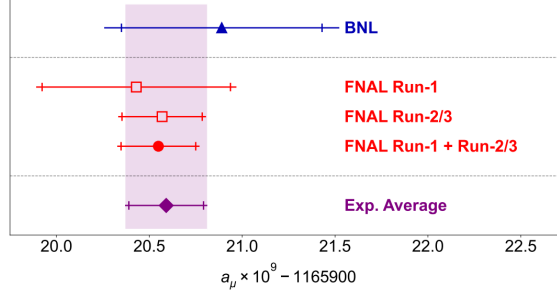
Figure 1: The magnetic anomaly of the muon (a_μ) measured at the BNL (blue triangle) and Fermilab (red points). The experimental average is predominantly set out by the new result by Fermilab collaboration [2]. The tickmarks indicate the statistical uncertainties.

The anomaly is obtained from the following formula:

$$a_\mu = \frac{\omega_a}{\tilde{\omega}'_p(T_r)} \frac{\mu'_p(T_r)}{\mu_e(H)} \frac{\mu_e(H)}{\mu_e} \frac{m_\mu}{m_e} \frac{g_e}{2}, \tag{1}$$

where only the first term $\mathcal{R}'_\mu = \omega_a/\tilde{\omega}'_p$ is measured in the Muon $g - 2$ experiment. The other terms ($\mu'_p(T_r)$ is the magnetic moment of the proton in a spherical water sample measured at the reference temperature $T_r = 34.7\,°C$, $\mu_e(H)$ is the magnetic moment of the electron in the hydrogen bound-state, $m_{\mu,e}$ are the masses of the muon and electron, respectively, and g_e is the electron g-factor) are constants computed or measured by other experiments, whose net uncertainty is 25 ppb. ω_a, the nominator of the ratio $\mathcal{R}'_\mu$, represents the anomalous spin precession frequency of the muon. And $\tilde{\omega}'_p(T_r)$ is the proton Larmor frequency convoluted over the average muon distribution at the reference temperature as a measure of the magnetic field. In the ideal condition, this frequency is given by

$$\omega_a = a_\mu \frac{q}{m} B, \tag{2}$$

where B is the strength of the magnetic field in the storage ring. Therefore, to measure a_μ, one needs to measure both ω_a and the magnetic field. ω_p, the proton Larmor precession frequency, is measured to quantify the magnetic field. More details for the magnetic field measurement can be found in Ref. [3]. In the subsequent sections, we will briefly describe the measurement of ω_a.

2. Anomalous Spin Precession Frequency

Due to the parity-violating weak decay, the muon decay is self-analyzing. The high-energy decay positrons are preferentially emitted along the muon spins, so the number of detected positrons
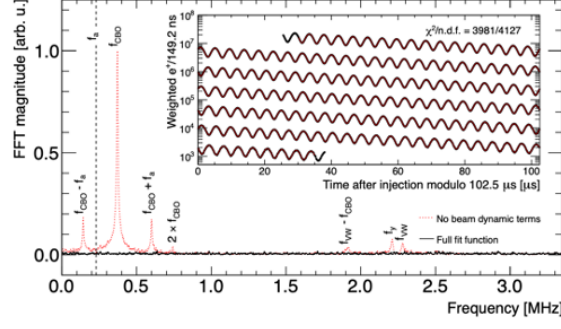
Figure 2: The inset figure represents the decay positron counts as a function of time modulo 102.5 μs, where the fit is overlaid in red. The figure shows the FFT spectrum of the residual between the data and the fit (red-dashed) without the beam dynamics terms ($\eta(t)$, see the text) and (black-solid) with them.

above some energy threshold oscillates at the spin precession frequency. The analysis is done by carefully modeling this oscillating exponential decay (dubbed "wiggle plot" in the Muon $g-2$ collaboration) and fitting to extract the frequency ω_a^m. We denote this as ω_a^m because this is uncorrected ω_a, as there are factors to be taken into account which affect ω_a due to the non-ideal beam motions, which will be dealt with in the next section. The basic fit functional form is

$$N(t) = N_0 \eta_N(t) e^{-t/\tau} \{1 + A\eta_A(t) \cos(\omega_a^m t + \phi_0 + \eta_\phi(t))\}, \tag{3}$$

where three $\eta(t)$ functions are the acceptance corrections due to the beam motions. More details can be found in Ref. [4]. The idea is to suppress the existing beam dynamics peaks in the wiggle plot to make sure ω_a^m is not biased, as shown in Fig. 2.

However, there are biases to ω_a that are not easily addressed by $\eta(t)$ terms. There are five such corrections, including those that have been known for a long time since one of the early muon $g-2$ experiments and those that were identified rather recently by extensive, accurate simulation studies:

$$\omega_a = \omega_a^m (1 + C_e + C_p + C_{pa} + C_{dd} + C_{ml}). \tag{4}$$

They are known as beam dynamics corrections since all of them originate from the non-ideal beam motions and their interplay with the external fields [5].

3. Beam Dynamics Correction to ω_a^m

There are two types of corrections, and the above five terms fall into either of them. One is due to the intrinsic bias to the ω_a, meaning that the muon spin actually precesses at a different rate. The E-field correction (C_e) and the pitch correction (C_p) are this type. The others, the phase-acceptance (C_{pa}), differential decay (C_{dd}), and the muon loss (C_{ml}) corrections, are the second type, where they effectively bias ω_a by inducing a time-varying phase. In this section, we will walk through the corrections one by one and highlight improvements since the first result. The values for the average beam dynamics corrections and their corresponding uncertainties for the first result (Run-1) and the latest result (Run-2/3) are summarized in Table 1.

Table 1: Average beam dynamics corrections in Run-1 and Run-2/3.

Beam Dynamics Corrections	Run-1	Run-2/3
C_e	508(53)	451(32)
C_p	180(13)	170(10)
C_{pa}	−154(75)	−27(13)
C_{dd}		−15(17)
C_{ml}	−11(5)	0(3)
Sum	523(93)	580(40)
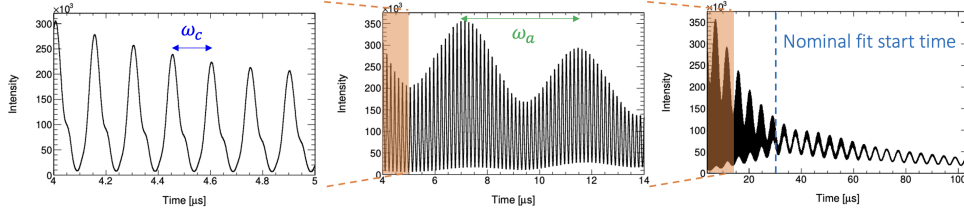
Figure 3: Illustration of the Fast Rotation. At the early time of the injection (< 30 μs), a fast 6.7 MHz cyclotron oscillation is pronounced due to a bunched beam. The Fast Rotation smears out as the beam debunches and gets uniformly distributed around the ring.

3.1 The E-field Correction C_e

Equation (2) holds for the ideal momentum muons in the storage ring. For an off-momentum muon, the equation of ω_a is given as

$$\omega_a \approx \frac{q}{m}\left[a_\mu B - \left(a_\mu - \frac{m^2}{p^2}\right)\frac{\beta E}{c}\right]. \tag{5}$$

The second term in the square brackets is canceled out for the ideal momentum, but in practice, the momenta are spread around the design value. So it induces a bias to ω_a in the presence of the electric field. The electric field is essential in the muon $g - 2$ storage ring to vertically focus the beam [6]. The E-field correction can be obtained by computing

$$C_e = 2n(1 - n)\beta_0^2\frac{\langle x_e^2\rangle}{R_0^2}, \tag{6}$$

where n is the weak focusing field index, β_0 is the ideal muon velocity, R_0 is the storage ring radius ($= 7.112$ m) and x_e is equilibrium radii of the stored muons.

The equilibrium radius distribution is measured primarily by the Fast Rotation analysis. The Fast Rotation refers to a prominent 6.7 MHz cyclotron frequency oscillation in the early time of the injection. This is because the beam is longitudinally bunched at the time of injection. As the beam debunches due to mixed cyclotron frequency according to the momentum spread, the Fast Rotation smears out and is much less pronounced 30 μs after the injection. This is illustrated in Fig. 3.

The dominant systematic error source for the E-field correction comes from the correlation between the injection time and the momentum distribution of stored muons. In Run-2/3, a bunch-level analysis was performed to sort out the effect of this injection-time-momentum correlation, and
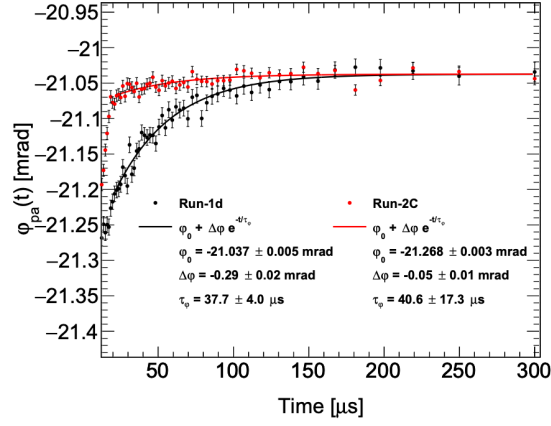
Figure 4: Phase-acceptance phase as a function of time after injection in Run-1 and Run-2. Due to the damaged electrostatic quadrupole resistors in Run-1, the early-to-late change in the average $g - 2$ phase is more significant in Run-1.

a complementary tracker-based analysis was conducted. As a result, the uncertainty was reduced by 40% compared to Run-1.

3.2 The Pitch Correction C_p

The pitch correction is induced by the vertical motion of the muon, which drives an out-of-plane precession at the vertical betatron oscillation frequency. The pitch correction can be obtained from the formula:

$$C_p = \frac{n}{2} \frac{\langle y^2 \rangle}{R_0^2} = \frac{n}{4} \frac{\langle A_y^2 \rangle}{R_0^2}, \tag{7}$$

where A_y is the vertical betatron oscillation amplitude. The amplitude distribution is measured by the tracker and calorimeter analysis. The trackers consist of ionization chamber straws filled with an Ar-Ethane gas. There are 8 modules at each of two tracker stations, aligned toward a nearby calorimeter. Using the position and momentum information when the positrons hit the straw modules, one can extrapolate the trajectory to find out the positional distribution of the decaying muons. More details of the trackers can be found in Ref. [7].

3.3 The Phase-Acceptance Correction C_{pa}

The phase-acceptance correction arises because the $g - 2$ phase of the accepted positrons depends on the muon decay position and energy. This itself, however, does not bias ω_a unless the average beam profile changes over time. The beam profile does change due to, for instance, slow decoherence of the coherent transverse betatron oscillations. In Run-1, the phase-acceptance effect was significantly enhanced due to damaged resistors in the electrostatic quadrupole system. The damaged resistors were replaced before Run-2 operation. Figure 4 shows a substantial difference between the average phase in Run-1 and Run-2.

3.4 The Differential Decay Correction C_{dd} and The Muon Loss Correction C_{ml}

There are other sources of the $g - 2$ phase to be time-varying. It turned out that the time dependence of the phase is induced by a combination of two effects: the phase-momentum correlation

and the momentum-time correlation. Namely,

$$\frac{\mathrm{d}\phi}{\mathrm{d}t} = \frac{\mathrm{d}\phi}{\mathrm{d}\langle p \rangle} \frac{\mathrm{d}\langle p \rangle}{\mathrm{d}t}. \tag{8}$$

There are three sources for the phase-momentum correlation: one from the upstream beamline dipole bending magnet, another from the injection p-x correlation, and the other from the head-to-tail p-t_0 correlation, where t_0 is the injection time. There are two sources for the momentum-time correlation: differential decay due to the momentum spread and momentum-dependent muon loss due to the dispersion effect. The correction from the former is the differential decay correction C_{dd}, and from the latter is the muon loss correction C_{ml}. These corrections are relatively smaller than the other corrections, but extensive simulation studies and analyses were performed to understand the effects. In Run-1, we didn't evaluate the differential decay systematics because the beamline C_{dd} was negligible compared to C_{ml}, which was enhanced due to the damaged resistors, and we were at the early stage of understanding the other sources of C_{dd} effect.

4. Conclusion

We present the beam dynamics corrections to the anomalous spin precession frequency ω_a^m in the Muon $g-2$ experiment at Fermilab. There have been a lot of improvements since our first result (Run-1), and the net systematic uncertainty of the beam dynamics correction terms was reduced by more than a factor of two in the latest result (Run-2/3).

References

[1] Muon $g-2$ collaboration, *Measurement of the positive muon anomalous magnetic moment to 0.46 ppm*, *Phys. Rev. Lett.* **126** (2021) 141801.

[2] Muon $g-2$ Collaboration collaboration, *Measurement of the positive muon anomalous magnetic moment to 0.20 ppm*, *Phys. Rev. Lett.* **131** (2023) 161802.

[3] Muon $g-2$ collaboration, *Magnetic-field measurement and analysis for the muon $g-2$ experiment at fermilab*, *Phys. Rev. A* **103** (2021) 042208.

[4] Muon $g-2$ collaboration, *Measurement of the anomalous precession frequency of the muon in the fermilab muon $g-2$ experiment*, *Phys. Rev. D* **103** (2021) 072002.

[5] Muon $g-2$ collaboration, *Beam dynamics corrections to the run-1 measurement of the muon anomalous magnetic moment at fermilab*, *Phys. Rev. Accel. Beams* **24** (2021) 044002.

[6] Y.K. Semertzidis et al., *The brookhaven muon (g2) storage ring high voltage quadrupoles*, *Nucl. Instrum. Meth. A* **503** (2003) 458.

[7] T.S. Stuttard, *The development, testing and characterisation of a straw tracking detector and readout system for the fermilab muon g-2 experiment*, .